Marine Predators Algorithm Based Stable Approximants Of Linear-Time Invariant Continuous-Time Systems

¹Chhabindra Nath Singh, ²Shekhar Gehlaut, and ³Akhilesh Kumar Gupta

¹Department of Electrical Engineering, Harcourt Butler Technical University, Kanpur-208002, India

²Department of Electrical Engineering, Motilal Nehru National Institute of Technology Allahabad, Prayagraj-211004, India

³Department of Electrical Engineering, BNCET, Lucknow, India E-mail: ¹cnsinghhbti7@gmail.com, ²gehlaut.shekhar@gmail.com,

³akhileshgupta08@gmail.com

Abstract:

In this article, a novel amalgamated model reduction method is proposed to simplify complex continuous-time systems using the Marine predators optimization algorithm (MPOA). The suggested approach guarantees the stability of the approximant since the stability equation approach is assimilated with MPOA. To prove the efficacy of the proposed method two case studies are considered. Additionally, this study includes a comparative examination of the dynamic responses and performance indices to support the superiority of the proposed method in comparison to existing approaches.

Keywords: Continuous-time systems, Model order reduction, Marine Predators Optimization Algorithm, Performance indices.

1. Introduction

The mathematical representation of complicated physical systems yields a model of significant complexity. Such a complex model increases the complication in control design and implementation. High-order control systems are often

comprise of intricate mathematical models that incorporate a multitude of state variables and parameters. The computing demands and time requirements of simulating or solving these models with high dimensions might be substantial. In addition, Real-time control is of utmost importance in various engineering domains, including aerospace, robotics, and autonomous vehicles. The implementation of high-order control systems in real-time scenarios may be deemed unsuitable due to the significant computational burden they entail. Hence, there is often a need for a reduced model that maintains a decent level of accuracy. Model order reduction (MOR) is a technique employed to simplify intricate models and decrease the computing burden associated with simulation. Since its inception, the utilization of MOR has been observed in a multitude of engineering applications (Jazlan et al., 2014; Sonker et al., 2017; Sonker et al., 2019). The objective of MOR is to decrease the intricacy of a model while preserving its fundamental dynamic characteristics. The decrease in complexity results in notable enhancements in computational efficiency, hence enabling the execution of real-time simulations, control design, and analysis. The act of decreasing the model order facilitates expedited execution of the control loop, hence enhancing the system's ability to promptly adapt to variations in conditions and disturbances. In addition, the process of designing and optimizing controllers for systems with a high order can present significant challenges and consume a considerable amount of time. Engineers can benefit from the reduction of model order since it allows them to work with reduced representations that are more amenable to analysis and manipulation. The process of simplification enhances the ease of designing and fine-tuning controllers, resulting in control strategies that are more efficient and effective. Reducedorder models offer a more concise depiction of the system, facilitating the integration and handling of uncertainty. This holds significant importance in the context of robust control and adaptive control applications.

The primary goals of MOR encompass three key aspects: (i) simplifying the assessment of system behavior, (ii) mitigating computing challenges, and (iii) devising a more simplified controller design. Over the past five decades, numerous MOR

strategies have been proposed for various classes of systems. One of the traditional methods for model order reduction (MOR) is the Padé approximation, first introduced by Shamash in 1974 (Shamash, 1974). Other commonly used techniques are the continuing fraction expansion (Shamash, 1976), time-moment matching (TMM) (Zakian, 1973), and so on. The methods (Shamash, 1974; Shamash, 1976; Zakian, 1973) have been seen to rely on algebraic computations and do not incorporate a stability condition. Therefore, it is possible that these methods may yield unstable approximants in certain instances, notwithstanding the stability of the actual system. Therefore, stability preserving methods (SPMs) (Chen et al., 1979; Choudhary and Nagar, 2019) are developed to overcome the instability issue considering different stability criteria. Moreover, a variety of mixed methods that combine traditional approaches with SPMs are presented in the existing literature so as to enhance the accuracy of approximation errors. The utilization of mixed approaches (Biradar et al., 2016; Vasu et al., 2016; Singh et al., 2019; Potturu et al., 2021) involves the application of a SPM for the computation of the denominator in a reduced-order approximant (ROA). In contrast, a conventional MOR approach is employed to estimate the numerator polynomial of the ROA. Subsequently, numerous researchers effectively applied various optimization strategies in conjunction with multi-objective optimization algorithms, taking into account a designated performance index as the fitness function. Several strategies have been proposed in the literature for addressing this problem. These includes the Salp Swarm Optimization (SSO) based strategy as presented by Ahamad and Sikander (2021), the Cuckoo search-based method as investigated by Gupta et al. (2018; 2019b) and Singh et al. (2018), and the Big Bang-Big Crunch (BB-BC) based approaches (Gupta et al., 2019a; Gupta et al., 2021; Jain & Hote, 2021; Singh et al., 2019), differential evolution based technique (Singh et al., 2021) and so on. Few researchers (Sikander and Prasad, 2015; Butti et al., 2021) employed only optimization algorithms for finding a ROA. It is also found that some of the avaiable methods such as (Biradar et al., 2016; Ahamad & Sikander, 2021; Jain & Hote, 2021; Potturu et al., 2021) do not always guarantee the stability of the obtained reduced order model.

Furthermore, the no free lunch theorem argues that it is not possible for one specific optimization technique to effectively solve all problems. Hence, the present study suggests a novel approach for MOR of higher-order continuous-time systems (HOCTS) that employs MPOA suggested by Faramarzi et al. (2020). The MPOA is inspired by the hunting and foraging behaviors of marine predators and has found applications in a variety of technical and scientific areas. These applications include, for example, in control systems and robotics for controller tuning and design for robotic systems Yakout et al. (2021), for trajectory planning of autonomous vehicles and drones (Cuevas et al., 2020), and for the path planning of robots (Yang et al., 2022), such as swarming robots. In addition, the algorithm also finds its applications in electrical engineering for circuit design and optimization, power system analysis and optimization (Sobhy et al., 2021), antenna design and placement in wireless communication systems (Owoola et al., 2023), to name a few. These applications demonstrate the versatility of the Marine Predator Optimization algorithm in tackling optimization and search problems across a wide range of scientific and technical disciplines, making it a valuable tool for researchers and engineers seeking efficient solutions to complex problems in various domains. This serves the main motivation for the selection of MPOA for the present study. The novelties and the main contributions of the proposed work are as presented below:

- (i) The proposed method guarantees the stability of the ROA if the original HOCTS is stable since the stability equations (Chen et al., 1979) are employed along with the MPOA (Faramarzi et al., 2020).
- (ii) The stability failure of the ROAs by Biradar et al. (2016), Ahamad & Sikander's method (2021), Jain & Hote (2021), and Potturu et al. (2021) is exhibited by considering two numerical examples. Apart from this, the problems associated with Sikander & Prasad's method (2015) and Butti et al.'s method (2021) are also highlighted.
- (iii) The effectiveness of the proposed strategy is demonstrated by incorporating a comparative analysis of the time and frequency domain findings from the two case studies.

2. Statement of the problem

Let an nth order linear-time invariant (LTI) stable HOCTS as

$$G_0(s) = \frac{N(s)}{D(s)} = \frac{\sum_{i=0}^{m} b_i(s)^i}{\sum_{j=0}^{n} d_j(s)^j}$$
(1)

where m < n and the numerator and denominator coefficients of the higher order system (HOS) are represented as b_i , d_j respectively. The objective of this article is to determine a stable reduced-order continuous-time approximant (ROCTA) from $G_o(s)$ as

$$G_r(s) = \frac{N_r(s)}{D_r(s)} = \frac{\sum_{i=0}^q e_i(s)^i}{\sum_{j=0}^r f_j(s)^j},$$
(2)

where q < r and e_i , f_j are the coefficients of the numerator and denominator of the reduced-order model (ROM) which are subject to the minimization of the performance index, which measures the discrepancy between the responses of systems $G_o(s)$ and $G_r(s)$, which can be expressed as

$$J = w_1 \int_0^{t_f} (c - c_r)^2 + w_2 (e_{ss} - e_{ssr}) + w_3 \|G_0 - G_r\|_{\infty}$$
(3)

here, the step responses of the original HOCTS is shown by c whereas the step response of the proposed ROCTA is represented by c_r . The final time is denoted by t_f , and the steady-state errors of the HOCTS and proposed ROCTA are denoted by e_{ss} and e_{ssr} , respectively. Weighting factors are represented by w_1 , w_2 , and w_3 and the H_{∞} norm error is given by $\|G_0 - G_r\|_{\infty}$.

3. Failure of the Existing techniques

In this article, two numerical examples are considered to demonstrate the instability issue of reduced model by Biradar et al.'s method (2016), Ahamad & Sikander's method (2021), Jain & Hote (2021) and Potturu et al.'s method (2021). It is unveiled that the stability claim made by these methods (Biradar et al., 2016; Ahamad & Sikander, 2021; Potturu et al., 2021) is not always valid.

Example 1:

$$G_1(s) = \frac{0.0067s^5 + 0.6s^4 + 1.5s^3 + 2.016s^2 + 1.55s + 0.6}{0.067s^6 + 0.7s^5 + 3s^4 + 6.67s^3 + 7.93s^2 + 4.63s + 1}$$

Following Biradar et al.'s method (2016), the time moments are obtained as -6.393; -1.228; 0.6 and 2.9436. Therefore, the second-order ROA by Biradar et al.'s method (2016) is obtained as

$$G_{1_{l_{[Biradar et al., 2016]}}}(s) = \frac{17.2962 - 24.1921s}{1 + 0.856s - 3.1541s^2}$$
(4)

As per the Routh stability criterion, all entries of the first column of the Routh array must be non-zero and of the same sign for stability. A sign change in the first column of the Routh table of the denominator polynomial of $G_{1r}(s)$ [Biradar et al., 2016] can be clearly observed which leads to instability. Similarly, the second-order ROA by Potturu et al.'s method (2021) for $G_1(s)$ is given by

$$G_{1r_{[Potturi et al., 2021]}}(s) = \frac{-0.19023 + 0.2265s}{-0.31704 - 0.27139s + s^2}$$
(5)

There is a sign change in the first column of the Routh array of the denominator polynomial of G_{1r} [Potturi et al., 2021]. Further, the 2^{nd} order model by Jain & Hote's method (2021) for Example 1 is obtained as

$$G_{1_{T_{[Jain and Hote, 2021]}}}(s) = \frac{-0.0951 + 0.1331s}{-0.31704 - 0.27139s + s^2}$$
(6)

It is evident that $G_{1r[Jain\ \&\ Hote,\ 2021]}$ (s) is also unstable due to a right half pole. Similarly, the 2^{nd} order ROA by Ahamad & Sikander method (2021) for $G_1(s)$ is given by

$$G_{1r_{Ahamad \& Sikander, 2021}}(s) = \frac{23.3268 - 32.6264s}{1 + 0.8560s - 3.1541s^2}$$
(7)

For the reduced model for $G_{1r [Ahamad \& Sikander, 2021]}$ (s) in (7) there exists a pole at 0.7149 which is in the right half of the s-plane.

Hence, G_{1r} [Ahamad & Sikander, 2021] (s) is also unstable. Now, another example is considered for which these methods (Biradar et al., 2016; Ahamad & Sikander, 2021; Jain & Hote, 2021; Potturu et al., 2021) yield unstable approximants.

$$0.1s^{6} + 9.205s^{5} + 44.78s^{4} + 86.06s^{3} + 98.36s^{2} +$$

$$G_{2}(s) = \frac{66.79s + 22.39}{s^{7} + 11.95s^{6} + 60.45s^{5} + 166.7s^{4} + 267.7s^{3} + 246.6s^{2} +$$

$$118.6s + 22.39$$

The time moments for Example 2 are derived as follows: -223.3127; -54.0866; -12.4825; -2.3140; 1.00; 5.6364; 26.2634; 110.2344; and 450.7146. The instability of both the 2^{nd} and 5^{th} order approximants of Example 2 has been examined. Both are found to be unstable. The 2^{nd} and 5^{th} order ROAs obtained by Biradar et al.'s method (2016) are given by

$$\begin{split} G_{2r_{[Biradar\ et\ al.,\ 2016]}} &= \frac{3.9871s - 0.9060}{10.2327s^2 + 1.9864s - 1} \\ &\qquad \qquad (8) \\ G_{5r_{[Biradar\ et\ al.,\ 2016]}} &= \frac{0.6677s^4 + 18.76s^3 - 9.352s^2 + 21.23s - 7.295}{4.956s^5 + 13.38s^4 + 26.5s^3 + 20.9s^2 + 3.179s - 1} \\ &\qquad \qquad (9) \end{split}$$

The instability of the 2nd-order approximant (8) can be attributed to the presence of a pole at 0.2303 in the right half of s-plane. We can determine stability of the ROA (9) by using Routh table which is given as below

4.95	26.	3.1
6	5	79
13.3	20.	-1
8	9	
18.7	3.5	
586	494	
18.3	-1	
683		
4.57		
07		
-1		

2:

The presence of a sign change in the first column of the Routh array indicates that the fifth order approximant of Example 2, as determined by Biradar et al.'s technique (2016) is characterized by instability. The 2^{nd} and 5^{th} -order models obtained by Potturu et al.'s method (2021) for $G_2(s)$ are given by

$$G_{2r_{[Potturu\ et\ al.,\ 2021]}} = \frac{0.4203s - 0.09773}{s^2 + 0.1941s - 0.09773}$$
(10)

$$G_{5\tau_{[Porturu\ et\ al.,\ 2021]}} = \frac{0.7942s^4 + 1.721s^3 + 1.596s^2 + 1.108s - 0.2018}{s^5 + 2.7s^4 + 5.346s^3 + 4.217s^2 + 0.6414s - 0.2018}$$
 (11)

The 2nd and 5th-order ROAs as per the approach proposed by Jain & Hote's method (2021) are obtained as follows

$$G_{2r_{[Jain \text{ and Hote, } 2021]}} = \frac{0.2648s - 0.0489}{s^2 + 0.1941s - 0.09773}$$
(12)

$$G_{5_{r_{[Jain \text{ and Hote, 2021}]}}} = \frac{0.9961s^4 + 1.439s^3 + 2.007s^2 + 0.8072s - 0.1009}{s^5 + 2.7s^4 + 5.346s^3 + 4.217s^2 + 0.6414s - 0.2018}$$
(13)

and the approximants obtained by the method given by Ahamad & Sikander's method (2021) are as follows

$$G_{2r_{\text{[Ahamad and Sikander, 2021]}}} = \frac{4.26s - 0.9757}{10.23s^2 + 1.986s - 1}$$
(14)

$$G_{5\eta_{[Ahamad \& Sikander, 2021]}} = \frac{7.724s^4 + 0.3822s^3 + 22.09s^2 - 6.925s + 3.841}{4.956s^5 + 13.38s^4 + 26.5s^3 + 20.9s^2 + 3.179s - 1}$$
(15)

The generated ROAs in equations (10)-(15) exhibit instability due to the presence of sign changes in the first column of the Routh array. This observation verifies the instability of these approximations. Hence, it is clear that all four methods (Biradar et al., 2016; Ahamad & Sikander, 2021; Jain & Hote.,

2021; Potturu et al., 2021) may not guarantee stable ROAs for all HOCTS.

4. Proposed Method

This section focuses on the two steps involved in the suggested approach for achieving ROA. The stability equations (Chen et al., 1979) are utilized in the initial stage to ascertain the denominator polynomial of the suggested ROCTA. The second part of the process entails the calculation of the numerator polynomial through the utilization of MPOA, as described by Faramarzai et al. (2020). This computation is carried out with the objective of minimizing the performance indices outlined in equation (3). The procedure for acquiring the planned ROCTA is outlined as follows:

4.1 Computation of ROA for the denominator

The computation of the denominator polynomial for the proposed ROCTA is performed initially. Therefore, the n-th order denominator polynomial (1) may be divided into two distinct sets: one consisting of even powers of s and the other consisting of odd powers of s, as demonstrated below:

$$E(s) = d_0 \prod_{j=1}^{n_e} 1 + \left(\frac{s}{z_{s_j}}\right)^2$$
(16)
$$O(s) = b_0 s \prod_{j=1}^{n_0} 1 + \left(\frac{s}{p_{s_j}}\right)^2$$
(17)

where n_e and n_0 are the integer parts of n/2 and (n-1)/2, respectively. It can be observed that $z_{s_j}^2$ and $p_{s_j}^2$ increases monotonically. Therefore, it is possible to remove the terms with bigger magnitudes in order to obtain the denominator of the rth order ROA. The development of the new equations is undertaken as

$$E_{smose}(s) = d_0 \prod_{j=1}^{r_e} 1 + \left(\frac{s}{z_{s_j}}\right)^2$$
(18)

$$O_{smose}(s) = b_0 s \prod_{j=1}^{r_0} 1 + \left(\frac{s}{p_{s_j}}\right)^2$$
(19)

where $r_{\rm e}$ and $r_{\rm o}$ are the integer parts of r/2 and (r-1)/2, respectively. Thus, the denominator of the proposed ROCTA is obtained as

$$D_{smose}(s) = E_{smose}(s) + O_{smose}(s)$$
 (20)

4.2. Computation of ROA for the numerator

In this section, the computation of the reduced-order numerator approximant of the proposed technique is performed using the MPOA as presented by Faramarzi et al. in 2020. The MPOA employs a modeling approach that incorporates Lévy and Brownian motion patterns to simulate the movement of ocean predators. This is done in conjunction with an optimal encounter rate strategy within a marine ecosystem. During low concentration of targets, it uses Lévy movement, whereas Brownian motion is followed during ample target case. Similar to other optimization algorithms, the initial solution of MPOA is distributed uniformly in the search space as

$$x_0 = x_{\min} + rand(x_{\max} - x_{\min})$$
 (21)

where x_{max} and x_{min} are the upper and lower bounds of the unknown variables and $rand \in [0,1]$ is a uniform random vector. As MPOA is based on the survival of the fittest, the best solution is entitled as the best predator. It forms an élite matrix which is given by

$$\acute{E}lite = \begin{bmatrix}
\acute{E}_{1,1}^{I} & \acute{E}_{1,2}^{I} & \cdots & \acute{E}_{1,d}^{I} \\
\acute{E}_{2,1}^{I} & \acute{E}_{2,2}^{I} & \cdots & \acute{E}_{2,d}^{I} \\
\vdots & \vdots & \vdots & \vdots \\
\acute{E}_{n,1}^{I} & \acute{E}_{n,2}^{I} & \cdots & \acute{E}_{n,d}^{I}
\end{bmatrix}_{n \times d}$$
(22)

where \vec{E}^I represents the best predator vector which constructs the Élite matrix by replicating n times, n is the number of search agents, and d is the number of dimensions. Based on the target's positions information, the arrays of this

matrix manage searching and finding the target. Both predator and target are considered search agents. The Élite matrix updates after each iteration if an improved predator replaces the best predator. The predators update their positions using the target matrix T. The initialization forms the initial target matrix, of which the best predator constructs the Élite matrix. The target matrix is given by

$$T = \begin{bmatrix} T_{1, 1} & T_{1, 2} & \cdots & T_{1, d} \\ T_{2, 1} & T_{2, 2} & \cdots & T_{2, d} \\ \vdots & \vdots & \vdots & \vdots \\ \vdots & \vdots & \vdots & \vdots \\ T_{n, 1} & T_{n, 2} & \cdots & T_{n, d} \end{bmatrix}_{n \times d}$$
(23)

where P_{i,i} presents the jth dimension of the ith target.

Considering different velocity ratios and imitating the life of a predator and target, the MPOA is separated into three main stages. A specific iteration period is specified and allocated for each stage which is as follows:

Stage 1 (The high-velocity ratio occurs when the predator exhibits a greater speed than its target): This phenomenon arises at the earliest stages of the optimization iterations. The mathematical representation of this stage is given as

while
$$Iter < \frac{1}{3}Iter_{max}$$

$$step \overrightarrow{size}_{i} = \overrightarrow{R_{B}} \otimes \left(\overrightarrow{Elite}_{i} - \overrightarrow{R_{B}} \otimes \overrightarrow{T_{i}} \right), \quad i = 1, 2, \cdots n$$

$$(24)$$

$$\overrightarrow{T_{i}} = \overrightarrow{T_{i}} + P.\overrightarrow{R} \otimes step \overrightarrow{size}_{i}$$

where $\overrightarrow{R_B}$ is the normal distribution-based random numbers vector that represents the Brownian motion and is denoted as P. The constant value of P is 0.5. R is a vector consisting of uniform random values within the range of [0, 1]. Iter refers to the current iteration, and iter_{max} is the maximum iteration.

The multiplication of $\hat{R_B}$ by target simulates the motion of the target.

Stage 2 (The unit velocity ratio refers to a scenario when both the predator and the target move at a same pace): This phase takes place during the intermediate optimization stage, wherein both the predator and the target actively search for their respective prey. Therefore, the objective of exploration is to transition towards exploitation. Consequently, one portion of the population is allocated for the purpose of exploration, while the remaining portion is designated for exploitation. During this phase, the prey organism engages in exploitation, while the predator organism engages in exploration. When a target exhibits Lévy motion with a unit velocity ratio ($v \approx 1$), the optimal strategy for a predator is to employ Brownian motion. The mathematical model pertaining to this particular step is

while
$$\frac{1}{3}Iter_{max} < Iter < \frac{2}{3}Iter_{max}$$

For the first half of the population:

$$\vec{stepsize}_{i} = \vec{R_{L}} \otimes \left(\vec{Elite}_{i} - \vec{R_{L}} \otimes \vec{T_{i}} \right); i = 1, 2, \dots, n/2$$

$$\overrightarrow{T_i} = \overrightarrow{T_i} + P.\overrightarrow{R} \otimes step \overrightarrow{size_i}$$
(25)

where $\overrightarrow{R_L}$ is a Lévy distribution based random number vector.

For the second half of the population:

$$stepsize_{i} = \overrightarrow{R_{B}} \otimes \left(\overrightarrow{R_{B}} \otimes \acute{E}lite_{i} - \overrightarrow{T_{i}}\right); i = n/2, \cdots n$$

$$\overrightarrow{T_{i}} = \acute{E}lite_{i} + P.CF \otimes stepsize_{i}$$
(26)

where
$$CF = \left(1 - \frac{Iter}{Iter_{max}}\right) \left(2 - \frac{Iter}{Iter_{max}}\right)$$
 is an adaptive

parameter which controls the predator movement.

Stage 3 (Low-velocity ratio: When predator moves faster than target):

This situation occurs in the last stage and associates with high exploitation. In a low-velocity ratio (v = 0.1), Lévy is the best strategy for a predator which is represented as

while
$$Iter > \frac{2}{3} Iter_{max}$$

$$stepsize_{i} = \overrightarrow{R_{L}} \otimes \left(\overrightarrow{R_{L}} \otimes \overrightarrow{Elite_{i}} - \overrightarrow{T_{i}}\right), \quad i = 1, \dots, n$$

$$\overrightarrow{T_{i}} = \overrightarrow{Elite_{i}} + P.CF \otimes stepsize_{i}$$
(27)

Here, the multiplication of $\overrightarrow{R_L}$ and Élite simulates predator movement in the Lévy scheme while adding the stepsize to Élite position simulates the predator movement to update target's position.

It is to be noted that the eddy formation or fish aggregating devices (FADs) cause behavioural change in Marine predators. The FADs may be considered as local optima, and a long-jump of predators avoids trapping into local optima. The effect of FADs is presented as

$$\overrightarrow{T}_{i} = \begin{cases}
\overrightarrow{T}_{i} + CF \left[\overrightarrow{X}_{\min} + \overrightarrow{R} \otimes \left(\overrightarrow{X}_{\max} - \overrightarrow{X}_{\min} \right) \right] \otimes U & \text{if } r \leq FADs \\
\overrightarrow{T}_{i} + \left[FADs(1-r) + r \right] \left(\overrightarrow{T}_{r1} - \overrightarrow{T}_{r2} \right) & \text{if } r > FADs
\end{cases}$$
(28)

where FADs = 0.2 is the probability of FADs effect on the optimization process, r is the uniform random number within

[0,1], The construction of $\vec{U} \in [0,1]$ involves the generation of a random vector, followed by the modification of its elements. Specifically, if an element in the vector is less than 0.2, it is set to zero, and if it is more than 0.2, it is set to one. The Pseudocode of the MPOA is given below

Initialize Target populations $i = 1, 2, \dots, n$

while termination criterion is not achieved

Calculate the fitness, construct the Élite matrix, and achieve memory saving

if Iter < Iter_{max} / 3 Update target using (24) elseif Iter_{max} / 3 < Iter < 2^* Iter_{max} / 3 For the first half of the populations $(i = 1, 2, \dots, n/2)$

```
Update target using (25)
For the second half of the populations (i = n/2, \dots, n)
Update target using (26)
elseif Iter > 2^* Iter<sub>max</sub> / 3
Update target using (27)
end if
Achieve memory saving and update Élite
Apply FADs effect and update using (28)
end while
```

5. Numerical Examples

The second-order reduced model for Example 1 is obtained using the proposed method which is given below:

$$G_{l_{smose}}(s) = \frac{0.076796 + 0.228345s}{0.1328 + 0.6146s + s^2}$$

The poles of the function $G_{1smose}(s)$ are located at -0.3073±0.19587j, which are situated in the left half of the complex s-plane. Therefore, it may be concluded that the aforementioned second-order reduced model exhibits stability. Table 1 displays the values of the integral square error (ISE), integral absolute error (IAE), integral of time multiplied absolute error (ITAE), and the H_{∞} norm error for Example 1. Additionally, the table includes the outcomes obtained using the existing methodologies (Biradar et al., 2016; Prajapati & Prasad, 2019b; Ahamad & Sikander, 2021; Jain & Hote, 2021; and Potturu et al.'s method, 2021).

According to the data presented in Table 1, it is evident that the suggested method yields the lowest values for ISE, IAE, and ITAE in comparison to other methods (Biradar et al., 2016; Prajapati and Prasad, 2019b; Ahamad & Sikander, 2021; Jain and Hote, 2021; Potturi et al., 2021). The proposed method yields a superior H_{∞} norm error compared to the methods proposed by Biradar et al. (2016), Ahamad & Sikander (2021), and Jain & Hote (2021). Nevertheless, the method proposed by Prajapati and Prasad (2019b) as well as the method presented by Potturu et al. (2021) exhibit a somewhat lower H_{∞} norm error compared to the strategy suggested in this

study. The instability of the second-order ROAs proposed by Biradar et al. (2016), Ahamad and Sikander (2021), Jain and Hote (2021), and Potturu et al. (2021) has been demonstrated in Section 3. Therefore, it is noteworthy that the error indices of the approximants derived from the methodologies employed by Biradar et al. (2016), Ahamad and Sikander (2021), Jain and Hote (2021), and Potturu et al. (2021) are significanty high.

The optimal values within the table are shown by the utilization of bold typeface. Additionally, Figures 1a, 1b, and 1c depict the step responses, error in step responses, and frequency responses, respectively, of the second-order approximations of Example 1 using both the proposed technique and Prajapati & Prasad's method (2019b). The Figures representing the plots for Biradar et al. (2016), Ahamad & Sikander (2021), Jain & Hote (2021), and Potturu et al. (2021) have not been generated due to the observed instability of the obtained results using these approaches. Based on the analysis of frequency responses, it is evident that the method proposed by Biradar et al. (2016) and the method proposed by Ahamad and Sikander (2021) do not yield a closely matched approximation. However, alternative approaches (Prajapati & Prasad, 2019b; Jain & Hote, 2021; Potturu et al., 2021), including the suggested method in this study, yield a satisfactory approximation.

Table 1: Comparison of various error indices of ROAs for Example 1

Method	$\left\ G-G_r ight\ _{\infty}$	ITAE	IAE	ISE
Proposed	0.3325559	1.412557	0.3649175	0.0307478
Ahamad &	22.72679	1.8732e+03	2.458138e+02	4.57792e+03
Sikander's (2021)				
Biradar et al.'s	16.69619	1.3689e+03	1.806033e+02	2.4711e+03
(2016)				
Jain & Hote's	0.3491158	51.33992	5.132514	4.161235675
(2021)				
Potturu et al.'s	0.323802	2.9526e+04	2.17084e+03	1.68447e+06
(2021)				
Prajapati &	0.292987	2.503519	0.7299123	0.103989638
Prasad's (2019)				

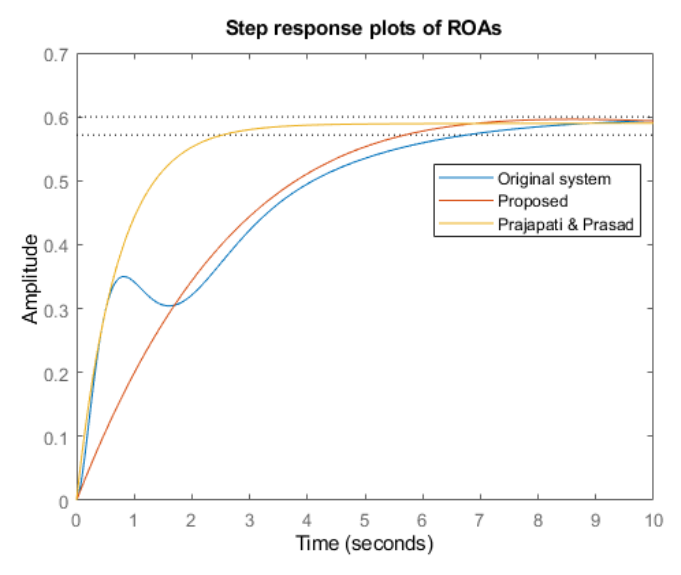


Fig. 1(a): Step response comparison

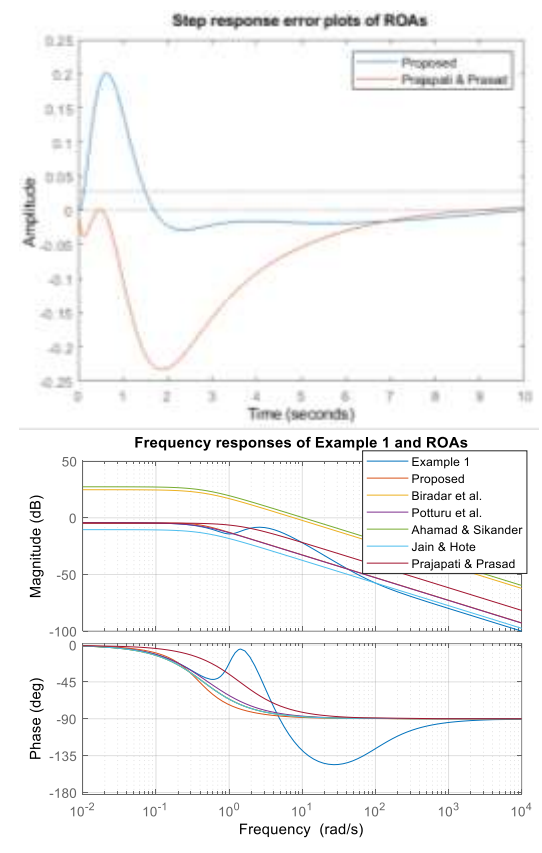


Fig. 1(b): Error in step responses

Fig. 1(c): Frequency response comparison

The 2nd and 5th-order approximants of Example 2 are analyzed, obtained by the proposed and existing methods

(Biradar et al., 2016; Prajapati & Prasad, 2019b; Ahamad & Sikander, 2021; Jain & Hote, 2021; Potturi et al., 2021). It is already shown in Section 3, that the 2nd and 5th-order ROAs obtained by Biradar et al. (2016), Ahamad & Sikander (2021), Jain & Hote (2021), Potturi et al. (2021) methods are unstable. The 2nd and 5th order approximations of Example 2, as calculated using the suggested method, are as follows:

$$G_{2_{smose}}(s) = \frac{0.33457s + 0.092096}{s^2 + 0.5145s + 0.0971}$$
 (29)

$$G_{5_{smose}}(s) = \frac{0.97035s^4 + 1.3592s^3 + 1.87817s^2 + 1.185s + 0.403407}{s^5 + 2.6359s^4 + 4.7695s^3 + 4.3961s^2 + 2.13s + 0.4021}$$

(30)

The poles of the system $G_{2smose}(s)$ are determined to be -0.25725 \pm 0.175847j. Therefore, it can be concluded that the second-order model for Example 2, as determined by the presented method, exhibits stability. In order to assess the stability of the suggested approximant (30), the Routh table is employed, as depicted in the following manner:

1	4.76	2.
	9	13
2.636	4.39	0.
	6	40
		21
3.101	1.97	
322	745	
	8	
2.715	0.40	
2392	21	
1.518		
18		
0.402		
1		

It is evident that there is an absence of sign change in the initial column of the Routh array. Therefore, it can be concluded that the suggested 5th-order ROA exhibits stability.

Hence, it can be concluded that the stability of the suggested method's ROAs in Examples 1 and 2 is established.

Table 2 presents the ISE, IAE, ITAE, and H_∞ norm error values obtained from the proposed technique and existing methods (Biradar et al., 2016; Prajapati & Prasad, 2019b; Ahamad & Sikander, 2021; Jain & Hote, 2021; Potturi et al., 2021) for Example 2. The method developed by Ahamad and Sikander (2021) demonstrates slightly superior results compared to the suggested method. However, when compared to the approaches presented by Biradar et al. (2016), Prajapati and Prasad (2019b), Jain and Hote (2021), and Potturi et al. (2021), the proposed method consistently achieves the lowest error indices.

Table 3 displays the error indices corresponding to the 5th order approximant of Example 2. The data shown in Table 3 indicates that Biradar et al. (2016) and Ahamad & Sikander (2021) exhibit higher error indices, which can be attributed to the presence of an unstable approximant, as discussed in Section 3. Remarkably, the method proposed by Potturu et al. (2021) yields reduced values of Integral Square Error (ISE), Integral Absolute Error (IAE), and Integral Time-weighted Absolute Error (ITAE) for the 5th-order approximant, even after having the presence of an unstable approximant. Nevertheless, the aforementioned methodologies (Biradar et al., 2016; Ahamad & Sikander, 2021; Jain & Hote, 2021; Potturi et al., 2021) do not provide a guarantee of the stability of the ROAs. In contrast, the proposed MOR method guarantees the stability of ROA and yields comparable error indices. Therefore, it can be inferred that, the proposed approach exhibits superior performance in comparison to the established methodologies (Biradar et al., 2016; Prajapati and Prasad, 2019b; Ahamad & Sikander, 2021; Jain & Hote, 2021; Potturi et al., 2021).

Table 2: Comparison of various error indices of 2nd-order ROAs for Example 2

Method	$\left\ G-G_r ight\ _{\infty}$	ITAE	IAE	ISE
Proposed	0.374959	2.0369210	0.4633578	0.0443109
Ahamad &	0.3461587865	0.78569923	0.31641214	0.02921412
Sikander's (2021)				

Biradar et al.'s	0.340750436	5.266572709	0.894394053	0.0675785051
(2016)				
Jain & Hote's	0.4996192342	24.59303554	3.562492821	0.9943055718
(2021)				
Potturu et al.'s	0.3463455085	9.71710739	1.053335375	0.11624444
(2021)				
Prajapati &	0.432037141	5.23155926	1.209650576	0.22484991
Prasad's (2019)				

Table 3: Comparison of various error indices of 5th-order ROAs for Example 2

Method	$\ G-G_r\ _{\infty}$	ITAE	IAE	ISE
Proposed	0.1195229	0.6216512	0.14269254	0.00267585
Ahamad & Sikander's	8.178719999	2.83356e+02	36.9070795	1.3019e+02
(2021)				
Biradar et al.'s (2016)	2.10059048	23.02517812	3.73066328	1.387690629
Jain & Hote's (2021)	0.499898171	52.5462873	0.27456137	3.06318055
Potturu et al.'s (2021)	0.1256661	0.18250369	0.0834931	0.0018081
Prajapati & Prasad's	0.17486613	0.1668596	0.10414799	0.00447967
(2019)				

The analysis of Figure 2a reveals that the proposed method provides a more accurate approximation compared to the approach presented by Prajapati & Prasad (2019b). However, there is room for improvement in the error of the step response in certain sections of the plot, as depicted in Figure 2b. In this case, all methods (Biradar et al., 2016; Prajapati & Prasad, 2019b; Ahamad & Sikander, 2021; Jain & Hote, 2021; Potturi et al., 2021) offers satisfactory frequency response characteristics. See Figure 2c. Figure 3 displays the plots of the fifth-order approximants, which bear resemblance to the plots observed in previous cases. The step responses depicted in Figure 3a provide clear evidence that, the suggested method closely approximates the response of the original system. However, it is worth noting that there is room for improvement in the step response error, as depicted in Figure 3b. This aspect should be explored further in future research endeavors. In the present scenario, it is seen that the frequency response estimate provided by Biradar et al. (2016) and Ahamad & Sikander's technique (2021) is inadequate for lower frequency ranges. Nevertheless, the proposed approach by Ahamad and Sikander (2021) offers an acceptable approximation for higher frequency values. In contrast, the method proposed offers a more accurate estimation across all frequency ranges. Hence, it can be inferred that the suggested approach guarantees the stability of the ROAs, a feature that was not guaranteed by previous methodologies (Biradar et al., 2016; Ahamad & Sikander, 2021; Jain & Hote, 2021; Potturi et al., 2021), while also offering comparable time and frequency response characteristics.

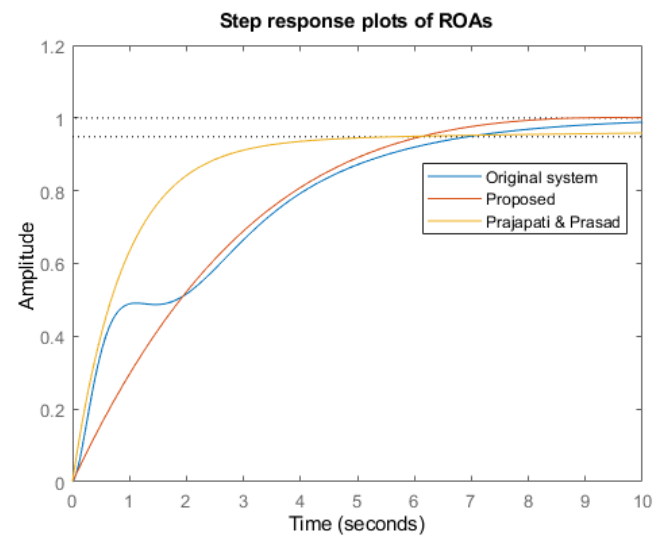


Fig. 2(a): Step response comparison

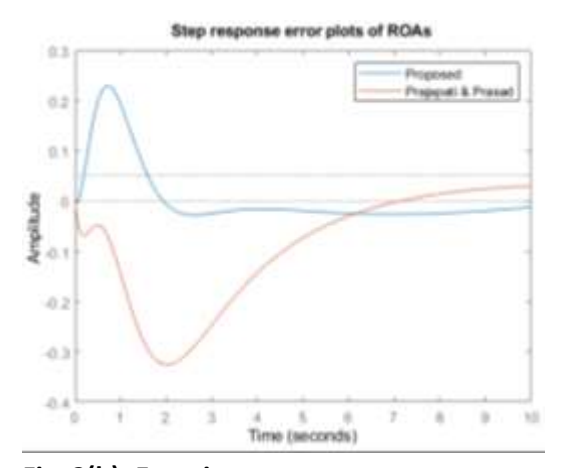


Fig. 2(b): Error in step responses

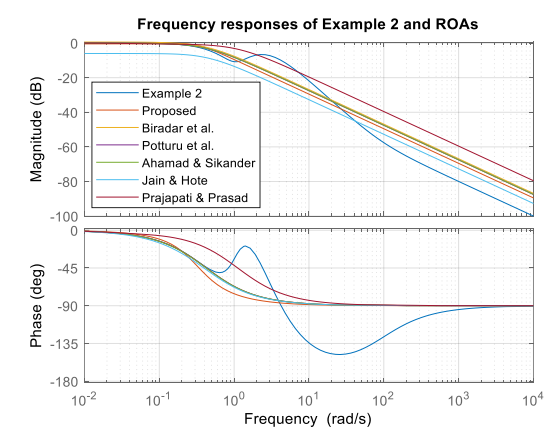
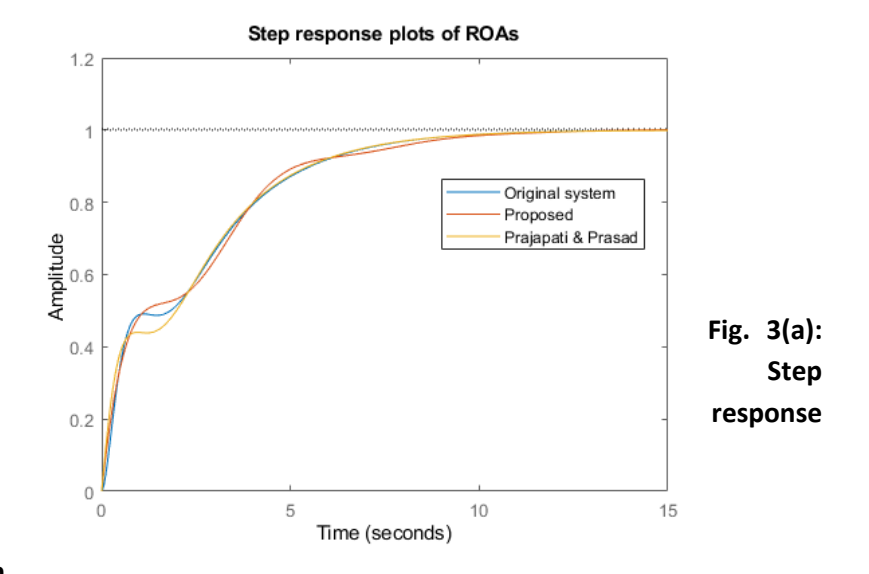
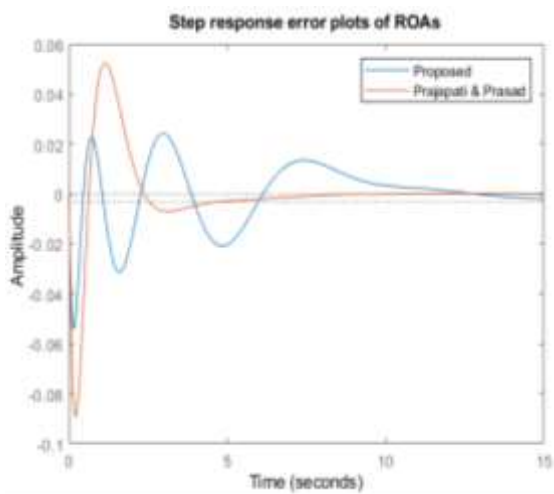


Fig. 2(c): Comparison of frequency responses



comparison



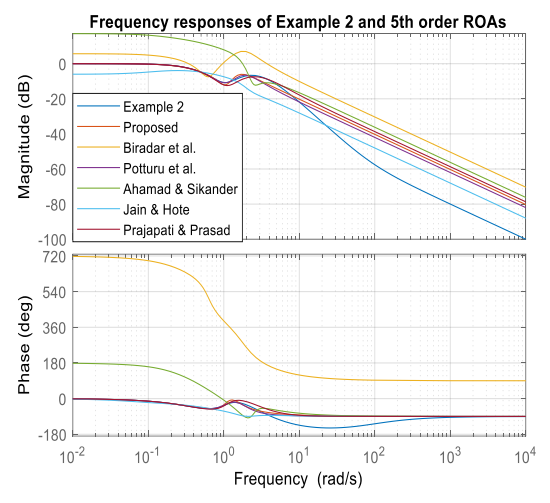


Fig. 3(b): Error in step responses

Fig. 3(c): Frequency response comparison

6. Conclusions

This article presents a novel approach for determining reduced-order approximations of higher-order continuous-time systems. The article also highlights the shortcomings and stability issues associated with existing methods (Biradar et al., 2016; Ahamad & Sikander, 2021; Jain & Hote, 2021; Potturi et al., 2021), as demonstrated through numerical examples. The proposed technique ensures the stability of all approximations if the original system is stable. Simulation results indicate that the proposed method generally provides a more accurate approximation compared to existing methods. However, it is worth noting that the simulation run-

time of the proposed method may be longer due to the fitness function, and there is room for improvement in terms of approximation error. Nonetheless, these limitations can be overlooked considering the stability guarantee offered by the proposed method, and these can be addressed in future research. Furthermore, the proposed method can be easily extended to discrete-time systems.

References

- A. Faramarzi, M. Heidarinejad, S. Mirjalili and Amir H. Gandomi (2020) 'Marine Predators Algorithm: A nature-inspired metaheuristic', Expert Systems with Applications, Vol. 152, pp. 1-28.
- Cuevas, F., Castillo, O., & Cortes-Antonio, P. (2022). A New Fuzzy Approach to Dynamic Adaptation of the Marine Predator Algorithm Parameters in the Optimization of Fuzzy Controllers for Autonomous Mobile Robots. In New Perspectives on Hybrid Intelligent System Design based on Fuzzy Logic, Neural Networks and Metaheuristics, pp. 179-204.
- Sobhy, M. A., Abdelaziz, A. Y., Hasanien, H. M., & Ezzat, M. (2021). Marine predators algorithm for load frequency control of modern interconnected power systems including renewable energy sources and energy storage units. Ain Shams Engineering Journal, 12(4), 3843-3857.
- Yakout, A. H., Kotb, H., Hasanien, H. M., & Aboras, K. M. (2021). Optimal fuzzy PIDF load frequency controller for hybrid microgrid system using marine predator algorithm. IEEE Access, 9, 54220-54232.
- Owoola, E. O., Xia, K., Adewuyi, V. O., & Kanda, P. S. (2023). Concentric Circular Antenna Array Synthesis Using Advanced Marine Predator Algorithm. Progress In Electromagnetics Research C, 132, 145-157.
- Yang, L., He, Q., Yang, L., & Luo, S. (2022). A fusion multi-strategy marine predator algorithm for mobile robot path planning. Applied Sciences, 12(18), 9170.
- Biradar, S., Hote, Y.V. and Saxena, S. (2016) 'Reduced-order modelling of linear time invariant systems using big bang big crunch optimization and time moment matching method',. Applied Mathematical Modelling, Vol. 40, No. 15-16, pp. 7225-7244.
- Butti, D., Mangipudi, S. K. and Rayapudi, S. (2021) 'Model order reduction based power system stabilizer design using improved whale optimization algorithm', IETE Journal of Research, pp.1-20

- Chen, T. C., Chang, C. Y. and Han, K.W. (1979) 'Reduction of transfer functions by the stability-equation method', Journal of the Franklin Institute, Vol. 308, No. 4, pp. 389-404
- Choudhary, A. K. and Nagar, S. K. (2019) 'Order reduction techniques via Routh approximation: a critical survey', IETE Journal of Research, Vol. 65, No. 3, pp. 365-379.
- Gupta, A. K., Kumar, D. and Samuel, P. (2019) 'A mixed-method for order reduction of linear time invariant systems using big bangbig crunch and Eigen spectrum algorithm', International Journal of Automation and Control, Vol. 13, No. 2, pp.158-175.
- Gupta, A. K., Kumar, D. and Samuel, P. (2019) 'Order reduction of linear time-invariant systems using Eigen permutation and Jaya algorithm', Engineering Optimization, Vol. 51, No. 9, pp. 1626-1643.
- Gupta, A. K., Singh, C. N., Kumar, D. and Samuel, P. (2021) 'Modified Eigen permutation-based model simplification of LTI systems using evolutionary algorithm', In: Intelligent Algorithms for Analysis and Control of Dynamical Systems, Springer, pp. 41-49.
- Gupta, A.K., Kumar, D. and Samuel, P. (2018) 'A meta-heuristic cuckoo search and Eigen permutation approach for model order reduction', Sadhana, Vol. 43, No. 5, pp. 1-11.
- Jain, S. and Hote, Y.V. (2021) 'Order diminution of LTI systems using modified big bang big crunch algorithm and approximation with fractional order controller design', International Journal of Control, Automation and Systems Vol. 19, No. 6, pp. 2105-2121.
- Jazlan, A., Sreeram, V., Togneri, R. and Bettayeb, M. (2014) 'Time weighted model reduction of at plate solar collectors', In: 2014 4th IEEE Australian Control Conference (AUCC), pp.107-111.
- Potturu, S. R., Prasad, R. and Meshram, R. (2021) 'Improved simplification technique for LTI systems using modified time moment matching method', Sadhana, Vol. 46, No. 3, pp. 1-11.
- Prajapati, A. K. and Prasad, R. (2019) 'Order reduction in linear dynamical systems by using improved balanced realization technique', Circuits, Systems, and Signal Processing, Vol. 38, No. 11, pp. 5289-5303.
- Shamash, Y. (1974) 'Stable reduced-order models using Padé-type approximations', IEEE transactions on Automatic Control, Vol. 19, No. 5, pp. 615-616.
- Shamash, Y. (1976) 'Continued fraction methods for the reduction of constant-linear multi-variable systems', International Journal of Systems Science, Vol. 7, No. 7, pp. 743-758.
- Sikander, A. and Prasad, R. (2015) 'A novel order reduction method using cuckoo search algorithm', IETE Journal of Research, Vol. 61, No. 2, pp.83-90.

- Singh, C. N., Gupta, A. K., Kumar, D. and Samuel, P. (2018) 'Fuzzy C-means based model simplification using Jaya optimization algorithm', In: 2018 2nd IEEE International Conference on Power Electronics, Intelligent Control and Energy Systems (ICPEICES), pp. 881-885.
- Singh, C. N., Gupta, A. K., Kumar, D. and Samuel, P. (2019) 'Improved pole clustering based simplification of complex systems using big bang-big crunch optimization', In: 2019 IEEE Students Conference on Engineering and Systems (SCES), pp. 1-6.
- Singh, C. N., Kumar, D. and Samuel, P. (2019) 'Improved pole clustering-based LTI system reduction using a factor division algorithm', Int. Journal of Modelling and Simulation, Vol. 39, No. 1, pp.1-13.
- Singh, C. N., Gupta, A. K., Kumar, D. and Samuel, P. (2021) 'A mixed approach for model reduction using differential evolution and Eigen permutation', In: Intelligent Algorithms for Analysis and Control of Dynamical Systems, Springer, pp. 51-59.
- Sonker, B., Kumar, D. and Samuel, P. (2017) 'A modified two-degree of freedom-internal model Control configuration for load frequency control of a single area power system', Turkish Journal of Electrical Engineering & Computer Sciences, Vol. 25, No. 6, pp. 4624-4635.
- Sonker, B., Kumar, D. and Samuel, P. (2019) 'Dual loop IMC structure for load frequency control issue of multi-area multi-sources power systems', International Journal of Electrical Power & Energy Systems, Vol. 112, pp. 476-494.
- Vasu, G., Sivakumar, M., Raju, M. R. (2016) 'A novel method for optimal model simplification of large scale linear discrete-time systems', Int. J. Automation and Control, Vol. 10, No. 2, pp. 120-141.
- Zakian, V. (1973) 'Simplification of linear time-invariant systems by moment approximants', International Journal of Control Vol. 18, No. 3, pp. 455-460.